Assessment of DFT Functionals for QTAIM Topological Analysis of Halogen Bonds with Benzene

Alessandra Forni,[*,†] Stefano Pieraccini,*[*,†,‡] Davide Franchini,[‡] and Maurizio Sironi*[*,†,‡]

[†] Istituto di Scienze e Tecnologie Molecolari del CNR (CNR-ISTM) and INSTM UdR, Via Golgi 19, 20133, Milano (Italy)

[‡] Dipartimento di Chimica and INSTM UdR, Università degli Studi di Milano, Via Golgi 19, 20133, Milano (Italy)

ABSTRACT Halogen bonding, a noncovalent interaction between a halogen atom and a nucleophilic site, is receiving a growing attention in the chemical community stimulating a large number of theoretical investigations. The DFT approach revealed to be one of the most suitable methods owing to its accuracy and low computational cost. We report here a detailed analysis of the performance of an extensive set of DFT functionals in reproducing accurate binding energies and topological properties for the halogen bonding interaction of either NCX or PhX molecules (X = F, Cl, Br, I) with the aromatic system of benzene in the T-shaped configuration. It was found that the better performance for both sets of properties is provided by a small subset of functionals able to take into account, implicitly or explicitly (by inclusion of an additive pairwise

potential) the dispersion contribution, that is, ωB97X, M06-2X, M11, mPW2PLYP-D and B2PLYP-D3.

1. INTRODUCTION

Intermolecular interactions play a key role in supramolecular chemistry, one of the fastest growing research areas in chemistry with considerable impact in different fields spanning life and materials sciences.[1] Several interactions, including principally hydrogen bonding, but also cation- and anion-π interactions, electrostatic and exchange forces, metal−ligand interactions and π−π stacking, have been exploited in the past to assemble new supramolecular architectures with pre-determined geometrical features and specific functions. On the other hand, halogen bonding (XB), that is the interaction between a covalently bonded halogen atom X and an acceptor group A with nucleophilic character, according to the scheme DX/A, has only recently been explored as a powerful tool at disposal of the supramolecular chemist to direct assembly phenomena.[2,3] While its use in the real world is still at a very initial stage, especially in the solution phase, several examples of functional applications can be mentioned, including the control of electrical and magnetic properties,[4] nonlinear optics,[5-9] the separation of isomers,[10] catalysis,[11-17] anion binding in the solution and solid states,[18-20] drug design and in protein−ligand complexation.[21,22]

The scarce initial interest shown towards halogen atoms as potential sites to drive supramolecular assembly is probably to be ascribed to the common view of these atoms as spherical entities, neutral in dihalogens or negative in halocarbon moieties. On the contrary, as demonstrated by Politzer et al. on the basis of electrostatic potential (ESP) analysis,[23] the electron density distribution around a halogen atom covalently bonded to a Y atom is strongly anisotropic owing to the depopulation, with respect to the unbound atom, of the valence p_z

orbital placed along the direction of the Y–X bond and a concomitant increase of population of the p_x and p_y orbitals perpendicular to this bond. The charge redistribution associated with the Y–X bond formation therefore implies a charge reduction in the region outwards the halogen atom, along the Y–X bond direction, compensated by an increase of electron charge in a belt around the bond axis. As a result, the corresponding ESP maps show a positive region along the extension of the Y–X bond, denoted as σ-hole, which acts as a site for nucleophilic attack.[23,24] The maximum value of the ESP and the size of the positive region strongly depend on the electron-withdrawing capability of D and on the polarizability of the halogen atom. A good correlation has been generally observed between the values of the ESP on the σ-hole and the strength of the halogen bond interaction,[24,25] explaining the experimental observation that the XB strength decreases in the order X = I > Br > Cl > F according to the decreasing polarizability of the halogens in that order. Moreover, this model provides a simple explanation for the strong directionality characterizing halogen bonding, because the XB acceptors, located in the direction of the rather narrow region of the σ-hole, will tend to align along the Y–X bond direction.

An alternative but complementary approach to explain the origin of XB is based on the so-called lump-hole model,[26] which is connected with the topology of the Laplacian of electron density, $\nabla^2\rho(\mathbf{r})$, in the valence shell of the interacting atoms.[27] A formal connection between the two approaches has been provided by Tognetti and Joubert.[28] Atomic regions with positive/negative Laplacian are regions of charge depletion/concentration. Following Bader,[27] and quoting Koritsanszky and Coppens,[29] "If two reactants approach each other in a Lewis acid-base-type reaction, their relative orientation can be predicted by the Laplacian functions of their electron density. Charge concentrations/depletions of one molecule can be considered to be complementary to depletions/concentrations of the other". Topological analysis of the Laplacian

in the region of the halogen-bonded atoms reveals exactly the presence of a charge depletion region along the extension of the Y–X bond (the hole) and a charge concentration region on the acceptor species A (the lump), which face each other in the intermolecular regions, according to a "key and lock" arrangement. The topology of the Laplacian then summarizes all the main features of XB, namely, its electrophilic-nucleophilic character, its strong directionality and its energetic basis (the latter connected with the relationship existing between the Laplacian and the local potential and kinetic energy densities).

The importance of the lump-hole model is also connected with the implicit inclusion of both interacting species in the topological analysis of their electron density distribution, unlike the σ-hole concept which is more focused on the inherent properties of the isolated XB donor molecule. In this context, a recent investigation[30] showed that the stability of the halogen bonded complexes is also strongly influenced by the polarizabilities of the XB acceptor molecules, and in particular of their lone pairs or π-electron system, which determine their nucleophilicity degree. This indicates that the electrostatic contribution alone is not sufficient to explain strength and geometrical features of halogen bonded complexes.

The large body of computational studies performed during the last 10 years on XB and other σ-hole interactions has been recently reviewed.[31] In particular, some papers assessing the performance of density functionals in treating specifically XB, in both vacuo[32] and solution,[33] or different noncovalent interactions including XB[34] have been recently published. An interesting analysis of the angular dependence provided by different functionals in YX…XY halogen bonding, revealing remarkable deviations from the correct CCSD(T)/CBS behavior, has been reported.[35] The Bader's Quantum Theory of Atoms in Molecules (QTAIM)[27] has been shown to

be a powerful tool to characterize and interpret the physical nature of halogen bonding[36-43] and to quantify, through analysis of topological local properties and atomic energies, the cooperative effects involving XB together with other interactions, specifically the beryllium bond. [44] One of the merits of QTAIM consists in its applicability to both the ab initio and experimentally derived electron density distributions, allowing both a meaningful comparison between information derived from theory and experiment and their mutual validation. An example of such analysis concerning halogen bonding is reported in ref. 45.

Despite the large use of QTAIM in characterizing halogen bond interactions or, also, in excluding to categorize a given interaction as halogen bond, as in the case of selected R–F···N interactions,[46] little attention has been payed, within the DFT framework, to the influence exerted on the topological properties by the functional used to build up the electron density distribution to be analyzed. To the best of our knowledge, only one systematic investigation on the ability of different functionals to predict accurate values of local QTAIM properties of covalent and a few non-covalent bonds has been previously reported.[47] In QTAIM investigations, it is generally customary to adopt the same functionals described as the best performing ones by benchmark studies on accurate determination of interaction energies. As shown here, however, topological properties of different electron density distributions as obtained for a given system by using such optimal (from the energy point of view) functionals can show non-negligible differences, which can hamper a meaningful comparison between properties determined for different non covalent interactions or for a same interaction taken in different molecular environments. An assessment of the performance of different functionals, based upon comparison with the corresponding properties obtained on a reference, Coupled Cluster with Single and Double substitutions (CCSD) electron density distribution is highly desirable.

Based on the series of accurate calculations previously reported by us on the halogen bonding with the aromatic system of benzene in the T-shaped geometry, DX/π,[41,48] we present here the results of a QTAIM analysis performed on the different wave functions obtained on the NCX/π and PhX/π (X = F, Cl, Br, I) halogen bonded complexes using the CCSD approach and different DFT functionals including, in particular, the best performing ones as individuated in our previous investigation.[41,48] The importance of the specific kind of halogen bond here considered relies on its frequent occurrence in biological macromolecules. In the recent survey by W. Zhu and co-workers,[49] it was shown that among the 778 short DX/A contacts retrieved in high-quality structures of the PDB, up to 211 involved delocalized π electron systems as the XB acceptor partner. Important examples of biological XB involving C–Cl(Br)/π interactions have been individuated in the design of potent and bioavailable inhibitors of the enzyme fXa, a serine protease factor which has been shown to play a key role in the blood coagulation cascade.[50] In the present DX/π study, the D = CN and Ph groups have been chosen, respectively, owing to the electron-withdrawing character of the former, giving rise to relatively strong XB interactions, and to the fact that in most XB interactions halogen atoms are linked to aryl groups. A clear evidence of the presence of a charge depletion region in the Laplacian distribution outwards the halogen, along the extension of the C–X bond, is shown in Figure 1 for two exemplifying cases, NCCl and NCBr.

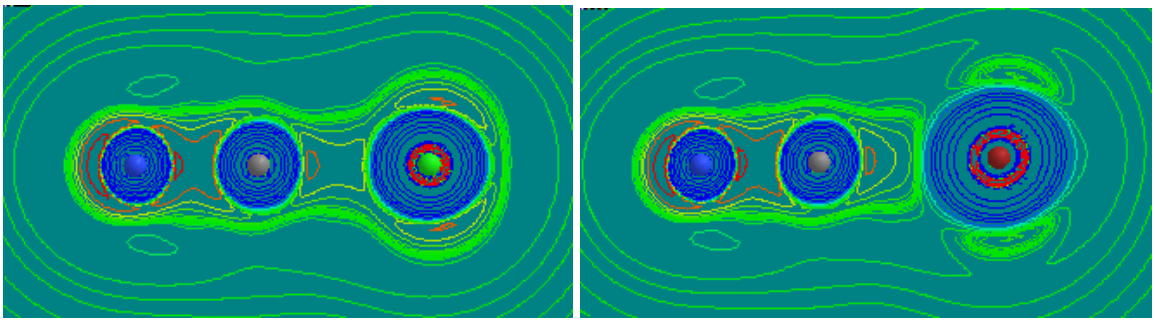

Figure 1. Laplacian of the CCSD/aug-cc-pVDZ electron density distribution of NCCl (left) and NCBr (right) molecules. The absolute values of the contours (au) increase in steps of 2×10^n, 4×10^n, and 8×10^n with n beginning at -3 and increasing in steps of 1. The scale of colors is: Red, contours with $\nabla^2\rho(\mathbf{r})) \leq -2$; Yellow, $-0.8 \leq \nabla^2\rho(\mathbf{r}) \leq -0.4$; Green, $\nabla^2\rho(\mathbf{r}) \leq |0.2|$; Cyan, $0.4 \leq \nabla^2\rho(\mathbf{r}) \leq 0.8$; Blue, $\nabla^2\rho(\mathbf{r}) \geq 2$.

2. COMPUTATIONAL DETAILS

The QTAIM topological analysis of the electron density distribution has been performed on the dimers of NCX and PhX (X = F, Cl, Br, I) with benzene in the T-shaped geometry. QTAIM reference values have been obtained on the wave functions obtained at the CCSD level of theory using the aug-cc-pVDZ basis set, which in the case of iodine included a pseudopotential to describe the core electrons.[51] For the latter atom, a core density has been accordingly added for the subsequent topological analysis of electron density. The geometries used for the CCSD calculations have been previously determined in our work, using the CCSD(T) method extrapolated to the complete basis set (CBS) limit.[41] For DFT calculations, full geometry optimization constrained to T-shaped geometry was carried out on the BSSE-free potential energy surface. Up to 17 functionals have been used to test their performance in reproducing both interaction energies and QTAIM properties related to the DX/π interaction, using as reference the CCSD(T)/CBS values previously published[41] and the presently reported CCSD values, respectively. In all cases, a large pruned integration grid (99 radial shells and 590 angular points per shell) has been used to avoid artifacts associated with numerical integration procedures, as evidenced by previous investigation on the sensitivity of functionals to the size of the integration grid.[52] This problem has been found particularly evident for meta-GGA

functionals, due to its dependence on the local kinetic-energy density in addition to the electron density and its gradient, which provided spurious oscillations in the potential energy curves unless very large integration grids are used.[53] The tested functionals have been chosen to cover different categories, that is: (i) the functionals based on the GGA with the add-on dispersion-correction term, B97-D[54,55] and B97-D3;[56,57] (ii) The hybrid GGA functionals (H-GGA), B3LYP,[58-60] B3PW91,[59,61,62] PBE1PBE (or PBE0)[63,64] and the recently developed APF and APF-D functional;[65] (iii) The range-separated or long-range corrected GGA functionals (LC-GGA), ωB97X[66] and ωB97X-D;[54,67] (iv) The hybrid meta-GGA functionals (HM-GGA), M05-2X,[68] M06-2X,[69] and M11;[70] and (v) The double hybrid GGA functionals (DH-GGA), B2PLYP,[58,71,72] mPW2PLYP,[73,74] B2PLYP-D,[75] B2PLYP-D3[56,72] and mPW2PLYP-D.[75] With respect to our previous work,[48] where we tested the ability of 34 functionals at reproducing the interaction energies of DCl or DBr (D=H, HCC, F, and NC) with the aromatic system of benzene, we have here excluded those characterized by the worse performance, except for the ubiquitously used B3LYP, while we have examined the performance of some recently developed functionals, that is APF, APFD and M11, and that of older functionals with the new DFT-D3[56] scheme to describe dispersion correction in DFT. It is worth to point out that the use of the Grimme pairwise dispersion correction has only an indirect effect on the electron density distribution. In fact, it consists in introducing an additive term to the standard Kohn-Sham energy while keeping unmodified the electron density. The latter turns out to experience the dispersion correction through its effect on the forces acting on nuclei and then on the molecular geometry, which will be modified (together with the associated electron density) with respect to the uncorrected case. On the other hand, the exchange and correlation energy expression of double hybrid GGA functionals include, through the MP2 correction term, non-local correlation effects responsible

for the dispersive interactions. However, since only part of the local GGA correlation energy, lacking attractive dispersion contributions, is replaced by the MP2 non-local correlation, it is found that these functionals generally underestimate the long-range dispersion. Addition of a DFT-D or DFT-D3 correction has been demonstrated to improve the performance of DH-GGA functionals for non covalent interactions.[72,75] It has been furthermore demonstrated that the functional form of the damping function, determining the short-range behavior of the DFT-D or DFT-D3 dispersion correction, has only minor impact on the results, provided a proper fitting of the damping parameters is performed.[57] In this connection, we mention that further improvement with respect to the original D[54] and D3[56] Grimme's damping parameters, used in the present work, has been afterwards obtained[76] by a refitting procedure based on a more extended benchmark set with respect to that previously used by Grimme. New databases covering a larger range of interaction energies and types have been used, and the existing ones have been extended to include more points of the potential energy surface along the radial direction, in particular at shorter intermolecular separations with respect to the equilibrium ones.

The QTAIM topological analysis of the CCSD and DFT electron density distributions was focused on the determination of local properties. The characterization of intermolecular interactions can be carried out by looking at the values of local properties at the bond critical points (BCPs) in the electron density $\rho(\mathbf{r})$,[77] that is, points at which $\rho(\mathbf{r})$ is minimum in the bond direction and maximum in perpendicular directions. Generally the BCP properties taken into consideration are the electron density, ρ_b, its Laplacian, $\nabla^2\rho_b$, the curvatures of $\rho(\mathbf{r})$ along the bond path, λ_3, and along directions perpendicular to such path, λ_1 and λ_2, the local potential, kinetic and total energy densities (V_b, G_b and $H_b = V_b + G_b$, respectively). Closed-shell interactions, such as the presently investigated weak halogen bonds, imply low ρ_b and positive

$\nabla^2\rho_b$, low curvatures λ_i, with the parallel curvature λ_3 largely dominating in magnitude the perpendicular ones, small local energy densities, with $2G_b > |V_b|$, and therefore positive and small total energy densities H_b. According to Espinosa et al.,[78] non bonded interactions can be classified on the basis of the $|V_b| / G_b$ ratio, which is <1 for closed-shell interactions and >2 for shared-shell interactions. When the ratio falls between 1 and 2, the interaction shows an intermediate character. Finally, the ratio of the perpendicular over the parallel curvature, $|\lambda_1| / \lambda_3$, provides further information for a classification of chemical bonding.[79] A curvature ratio <<1 is typical for closed-shell interactions, whereas $|\lambda_1| / \lambda_3 > 1$ has been found for shared interactions.

All calculations were performed using the Gaussian 09 Rev. D.01[80] suite of programs. The QTAIM topological analysis was performed with the AIMAll program.[81] It should be remarked[82] that the energetic properties as evaluated by AIMAll for DFT wavefunctions, both at local and integrated levels, suffer from the fact that the kinetic energy refers to a fictitious non-interacting system, missing the correlation term. This in principle would prevent to recover post-HF values even in the hypothetical case of exact exchange-correlation functional. Some approaches have been recently developed to overcome this difficulty within QTAIM, based on the use of either the virial theorem in the Kohn-Sham formalism[83] or density functional approximations for determining the correlation kinetic energy. [84,85]

3. RESULTS AND DISCUSSION

As reported in our previous investigation[41] on DX/π interacting systems (D = NC, Ph; X = F, Cl, Br, I) involving halogen atoms and the π-electron system of the benzene ring in the T-shape configuration, the underlying interaction is quite weak, in particular when the bonded group is the phenyl ring. Going from fluorine to iodine, the reference BSSE-corrected CCSD(T)/CBS

interaction energies ranged from -1.56 to -4.84 kcal/mol when D was the strongly electron-withdrawing CN group and from -0.42 to -2.87 kcal/mol for D = Ph, at intermolecular distances in the ranges 3.10 – 3.50 and 3.20 – 3.65 Å, respectively.[41] In all cases, however, an energy minimum on the DX/π PES was always detected, though the weaker interactions, i.e., those involving fluorine and/or the phenyl ring as D group, should be hardly viewed as halogen bonding due to the predominant contribution of dispersive forces with respect to the electrostatic ones, which prevail in the stronger interactions.[41] It should also be pointed out that fluorine has been included in the present analysis owing to its borderline role, giving rise to XB only when it is bonded to a strongly electron-withdrawing moiety.[86,87]

The reference values of the QTAIM topological properties, determined on the CCSD/aug-cc-pVDZ electron density distributions, are gathered in Table 1. In all cases, atomic interaction lines of maximum electron density (that is, bond paths being the systems at their equilibrium geometry) connecting the halogen atom with the six carbon atoms of the phenyl ring have been found (see Figure 2 for the molecular graphs of the bromine complexes), confirming that these atoms are chemically bonded according to QTAIM. In the case of the PhX/π systems, where the T-shaped approach of PhX to the benzene ring generates a slight asymmetry in the carbon atoms of the latter, negligible differences were found among the topological properties related to the four equivalent carbon atoms with respect to those determined for the other two carbons, therefore only average values have been considered in the present analysis.

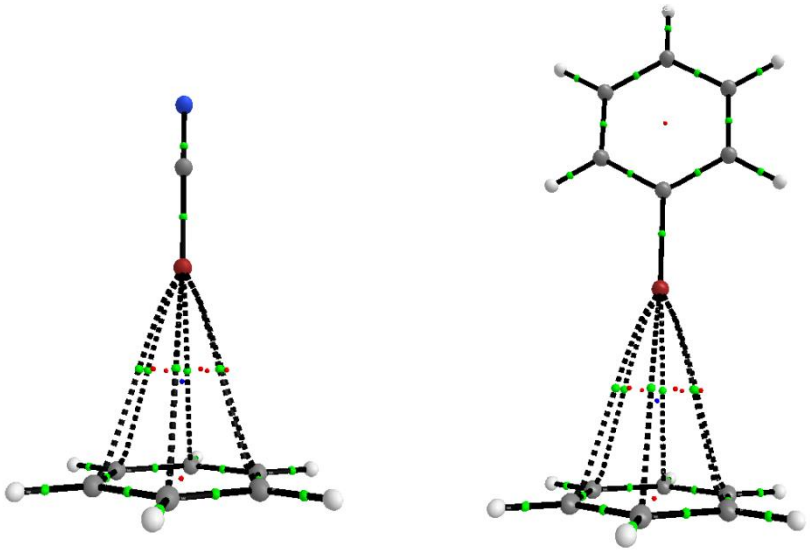

Figure 2. Molecular graphs of the complexes NCBr/π (left) and PhBr/π (right) obtained on the CCSD/aug-cc-pVDZ electron density distribution. Green/red circles correspond to bond/ring critical points.

Table 1. Bond critical point properties of the NCX/π and PhX/π (X=F, Cl, Br, I) interactions computed on the CCSD/aug-cc-pVDZ electron density distribution.[a]

DX	ρ_b	$\nabla^2\rho_b$	λ_1	λ_3	V_b	G_b	$\lvert\lambda_1\rvert/\lambda_3$	H_b	$\lvert V_b\rvert/G_b$
NCF	0.0036	0.017	-0.0022	0.0187	-0.00264	0.00338	0.116	0.00074	0.78
NCCl	0.0048	0.016	-0.0025	0.0185	-0.00271	0.00334	0.137	0.00063	0.81
NCBr	0.0050	0.015	-0.0023	0.0170	-0.00268	0.00317	0.137	0.00048	0.85
NCI	0.0053	0.015	-0.0025	0.0175	-0.00269	0.00321	0.141	0.00052	0.84
PhF	0.0031	0.014	-0.0018	0.0162	-0.00218	0.00288	0.112	0.00071	0.75
PhCl	0.0039	0.013	-0.0020	0.0146	-0.00222	0.00268	0.134	0.00047	0.82
PhBr	0.0041	0.012	-0.0019	0.0138	-0.00220	0.00257	0.141	0.00038	0.85
PhI	0.0044	0.012	-0.0020	0.0141	-0.00214	0.00257	0.143	0.00043	0.83

[a] Symbols denote BCP electron density, ρ_b; Laplacian of the density, $\nabla^2\rho_b$; Eigenvalues of the density Hessian matrix, λ_i; local potential, kinetic and total energy densities, V_b, G_b, and $H_b=V_b+G_b$, respectively. All quantities are expressed in a.u.

Despite the rather different interaction energies obtained for the series NCX with respect to the PhX one, the corresponding values of topological properties at the BCPs for a same halogen atom are fairly similar. In particular, the ρ_b values were in the ranges 0.0036-0.0053 a.u. for NCX systems and 0.0031-0.0044 a.u. for PhX systems. Such values are comparable with those commonly obtained for weak hydrogen bonds such as the DH/π interaction.[88-90] In all cases the positive sign of $\nabla^2\rho_b$ and the relationships $|\lambda_1| / \lambda_3 < 1$ and $|V_b| / G_b < 1$ confirm the closed-shell character of these interactions.

Up to 17 DFT functionals have been then tested to assess their ability at reproducing the values of interaction energy, equilibrium distance between the halogen atom and the plane of the benzene ring and topological properties at the BCPs. All the computed values of these properties are reported in Tables S1-S4 for the NCX/π systems and in Tables S5-S8 for the PhX/π systems (X = F, Cl, Br and I, respectively), together with the corresponding reference values. The ratios between the values obtained at the DFT level and the reference values, which provide an immediate indication of the deviations of the different DFT functionals from the reference, are given in Tables S9-S16. The corresponding MP2 values are also reported for completeness, confirming the previously noted tendency of this method to overestimate the strength of the interaction when delocalized π systems are involved.[91] This is particularly evident for the weaker PhX/π interaction. The topological analysis on the MP2 electron density distribution, on the other hand, provides BCPs properties in general very close to the CCSD reference.

All the functionals tested in the present work provided stable halogen-bonded dimers between NCX and benzene, while some functionals were not able to reproduce the binding for any or just a few dimers involving the PhX molecules. In particular, B3LYP and B3PW91 provided repulsive curves for all PhX/π dimers, APF for the dimers involving F, Cl and Br halogen atoms, and B2PLYP, M05-2X, M06-2X, M11, mPW2PLYP, PBE1PBE and ωB97X for only those involving fluorine. It is also noteworthy that, even in the cases where an attractive curve was obtained for the DF/π interaction (both D = NC and Ph cases), the values of ΔE_{CP} and equilibrium distance were characterized by large errors in several instances, owing to the well-known difficulty in accurately reproducing dispersive contributions by means of DFT approaches. For this reason the following discussion on the performance of the functionals in describing the DX/π halogen bonding on a statistical basis will be carried out both including and excluding the complexes with X = F, recognizing in the latter case that the term 'halogen bonding' is more appropriate only for the heavier halogen atoms.

Quick information about the performance of the functionals can be obtained by looking at the mean absolute relative errors, $\langle\varepsilon\rangle = \langle|(x - x_{ref}) / x_{ref}|\rangle$, computed on interaction energies, $\langle\varepsilon\rangle_{\Delta Ecp}$, and on the whole set of topological properties at the BCPs, $\langle\varepsilon\rangle_{QTAIM}$. They are reported in Table 2 and graphically shown in Figures 3 and 4 for $\langle\varepsilon\rangle_{\Delta Ecp}$ and $\langle\varepsilon\rangle_{QTAIM}$, respectively. The averages were performed on both separately the NCX/π and PhX/π systems, owing to their different energetic features, and on all systems, in all cases including and excluding the complexes with X = F as just commented. For the $\langle\varepsilon\rangle_{QTAIM}$ errors, the average was further performed on all the BCPs topological properties taken into consideration, where, in particular, we have considered separately V_b and G_b, and λ_1 and λ_3, rather than the related quantities, H_b =

$V_b + G_b$ or $|V_b|/G_b$ and $|\lambda_1|/\lambda_3$. The latter are in fact sometimes well determined only as a consequence of a compensation of errors when summing up or computing the ratio between V_b and G_b or between λ_1 and λ_3. This is evident by looking at the ratios between DFT and CCSD reference values (see Tables S9-S16), which are close to 1 even for the less performing functionals. The means were obviously computed only for the systems where an attractive interaction was determined, so that no errors are reported for the PhX/π interaction studied by B3LYP and B3PW91. Moreover, the worst functionals, as judged on the basis of their large $<\varepsilon>$ values (such as APF) should be considered even poorer because the reported errors do not take into account that they are not able to reproduce all the PhX/π bonded dimers.

Table 2. Mean absolute relative errors on interaction energies, $<\varepsilon>_{\Delta Ecp}$, and on the topological properties at the BCPs, $<\varepsilon>_{QTAIM}$, for the NCX/π, PhX/π and DX/π (D = NC and Ph) systems, including and excluding the cases with X = F, as obtained for the different DFT functionals.

	$<\varepsilon>_{\Delta Ecp}$						$<\varepsilon>_{QTAIM}$					
	NCX	NCX no F	PhX	PhX no F	DX	DX no F	NCX	NCX no F	PhX	PhX no F	DX	DX no F
MP2	0.10	0.11	0.24	0.21	0.17	0.16	0.03	0.03	0.05	0.05	0.04	0.04
B97D	0.10	0.13	0.18	0.19	0.14	0.16	0.17	0.12	0.25	0.16	0.21	0.14
B97D3	0.12	0.13	0.11	0.10	0.11	0.11	0.19	0.12	0.28	0.19	0.23	0.15
B3LYP	0.73	0.72	-	-	0.73	0.72	0.57	0.54	-	-	0.57	0.54
B3PW91	0.76	0.74	-	-	0.76	0.74	0.60	0.50	-	-	0.60	0.50
PBE1PBE	0.44	0.43	0.86	0.86	0.65	0.64	0.31	0.26	0.53	0.53	0.42	0.39
APF	0.59	0.56	0.90	0.90	0.75	0.73	0.42	0.35	0.55	0.55	0.49	0.45
APFD	0.20	0.19	0.20	0.12	0.20	0.16	0.06	0.06	0.05	0.06	0.06	0.06
ωB97X	0.09	0.04	0.11	0.11	0.10	0.07	0.09	0.10	0.08	0.08	0.09	0.09
ωB97XD	0.09	0.08	0.23	0.10	0.16	0.09	0.20	0.15	0.24	0.17	0.22	0.16
M052X	0.03	0.01	0.32	0.32	0.17	0.17	0.07	0.04	0.12	0.12	0.10	0.08
M062X	0.10	0.12	0.04	0.04	0.07	0.08	0.12	0.12	0.07	0.07	0.10	0.10
M11	0.08	0.09	0.13	0.13	0.11	0.11	0.07	0.05	0.03	0.03	0.05	0.04

B2PLYP	0.45	0.44	0.85	0.80	0.65	0.62	0.29	0.28	0.46	0.46	0.38	0.37
mPW2PLYP	0.29	0.31	0.71	0.61	0.50	0.46	0.25	0.25	0.38	0.38	0.31	0.32
B2PLYPD	0.03	0.04	0.23	0.21	0.13	0.13	0.05	0.05	0.08	0.08	0.06	0.06
B2PLYPD3	0.05	0.04	0.16	0.08	0.10	0.06	0.08	0.06	0.12	0.10	0.10	0.08
mPW2PLYPD	0.06	0.02	0.17	0.17	0.12	0.10	0.05	0.06	0.10	0.11	0.08	0.08

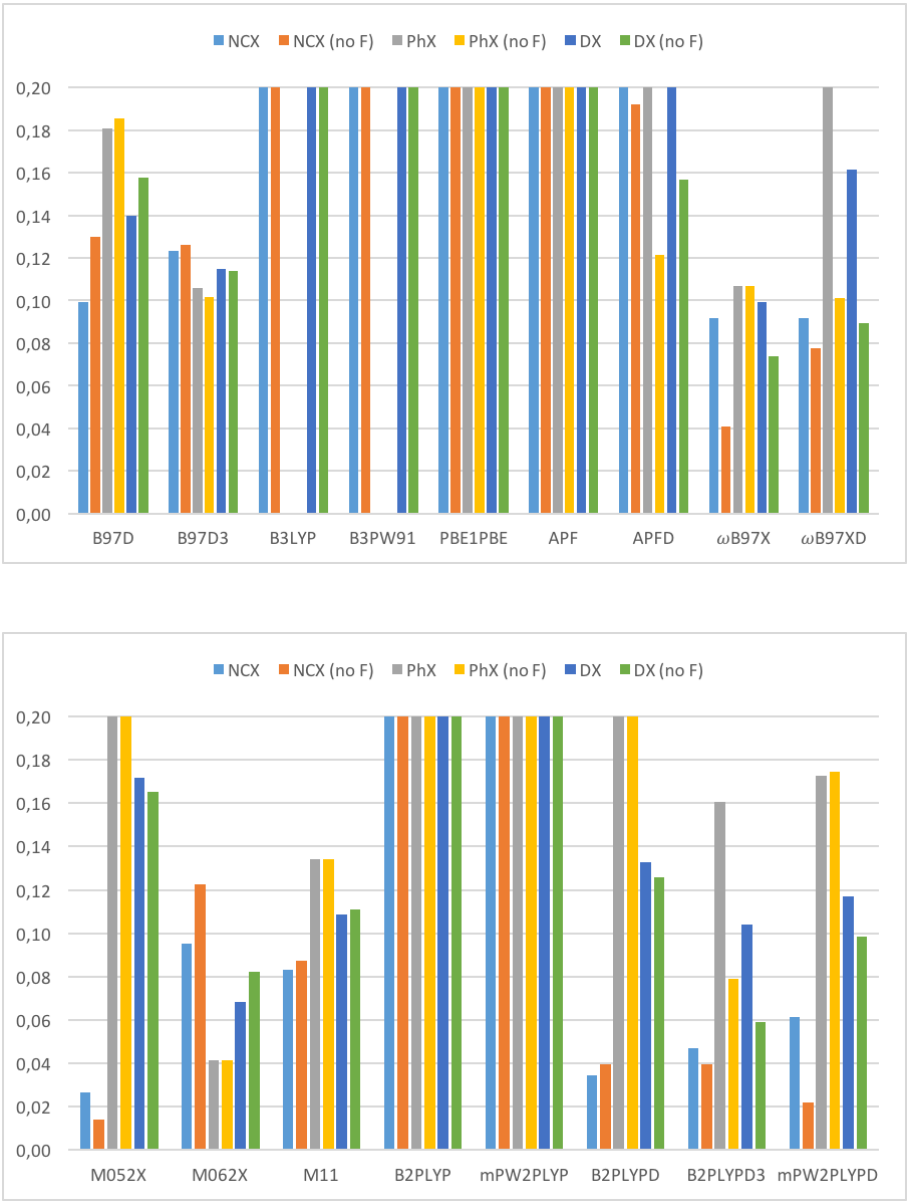

Figure 3. Mean absolute relative errors on interaction energies, $<\varepsilon>_{\Delta Ecp}$, for the different DFT functionals. Color of the bars means: Light blue, NCX/π; Orange, NCX/π excluding fluorine;

Gray, PhX/π; Yellow, PhX/π excluding fluorine; Blue, NCX/π and PhX/π; Green, NCX/π and PhX/π excluding fluorine. Missing bars denote that the functional does not reproduce bonded dimers.

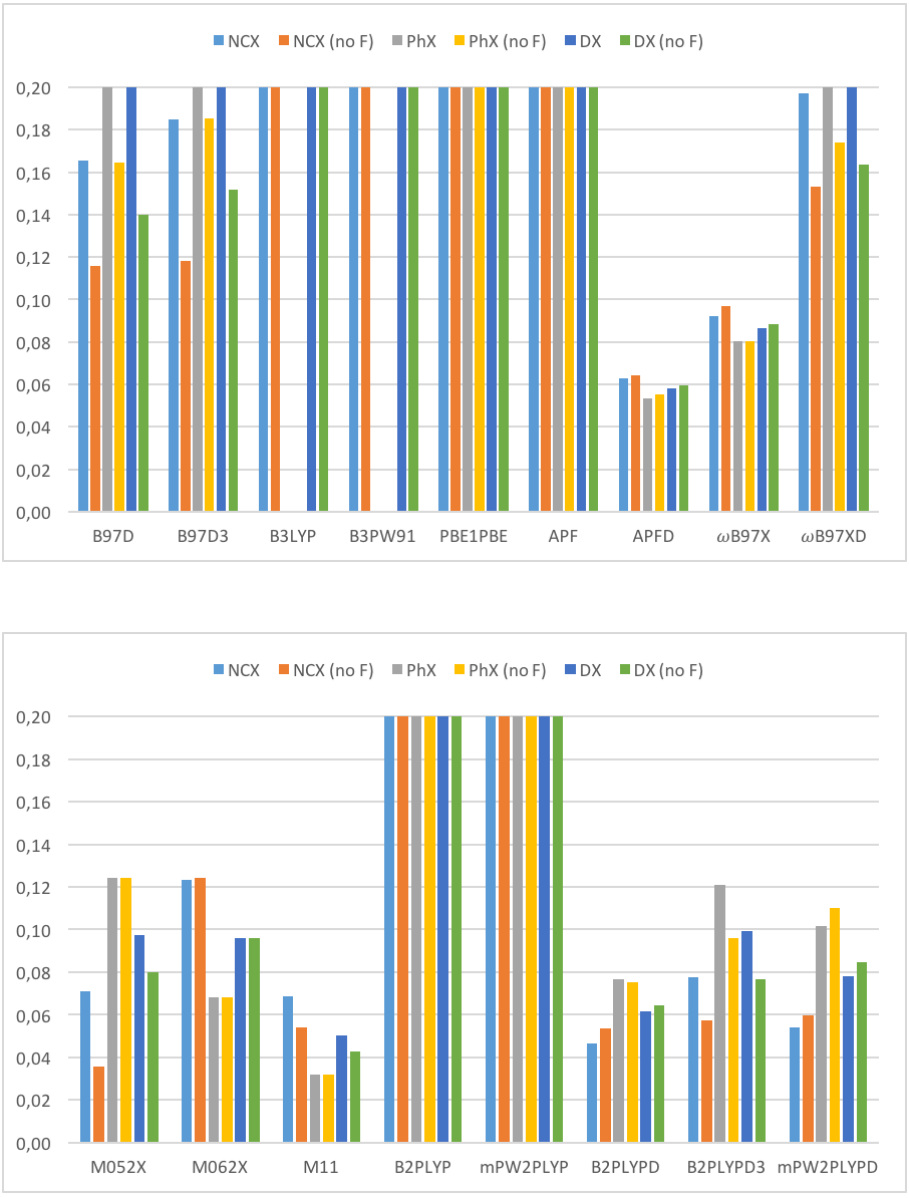

Figure 4. Mean absolute relative errors on topological properties at BCPs, $\langle\varepsilon\rangle_{QTAIM}$, for the different DFT functionals. Color of the bars means: Light blue, NCX/π; Orange, NCX/π excluding fluorine; Gray, PhX/π; Yellow, PhX/π excluding fluorine; Blue, NCX/π and PhX/π;

Green, NCX/π and PhX/π excluding fluorine. Missing bars denote that the functional does not reproduce bonded dimers.

Inspection of Figure 3 further supports, by inclusion of new functionals, our previous result[48] about the importance to include dispersion to treat the DX/π halogen bonding interaction. B3LYP, B3PW91, PBE1PBE, APF, B2PLYP and mPW2PLYP functionals provide in fact percentage $<\varepsilon>_{\Delta Ecp}$ errors well above an acceptable 20% threshold, even when able to give bonded dimers. This is particularly evident by comparing errors obtained for a same functional, with or without dispersion correction term. Results, in fact, greatly improve passing from APF to APF-D, from B2PLYP to B2PLYP-D or B2PLYP-D3 and from mMPW2PLYP to mPW2PLYP-D. The only unexpected 'anomaly' is represented by ωB97X which is on average superior to ωB97X-D, except for the fact that including the dispersion term permits to recover the binding also for the dimer involving PhF. It is to be pointed out that the present weakly bonded DX/π interacting systems should be somehow distinguished from the commonly investigated halogen bonds involving lone pairs, for which Kozuch and Martin[32] in their comprehensive study concluded that dispersion corrections provide a spurious overestimation of the XB strength. On the other hand, the role of dispersion in such more strongly interacting systems has been recently highlighted by Otero-de-la-Roza et al.,[92] who showed that dispersion correction, introduced in their work by means of the exchange-hole dipole moment (XDM) pairwise model,[93,94] improves the XB description provided a functional with low delocalization error is used. The authors demonstrate that such error is almost exclusively determined by the fraction of exact exchange in the adopted functional.

On the whole, only very few functionals provide percentage errors on energy below or slightly above 10%, also excluding the very weak interaction involving fluorine atom. They are the previously suggested ωB97X (7%), ωB97X-D (9%), M06-2X (8%) and mPW2PLYP-D (10%), and the presently tested B97-D3 (11%), M11 (11%) and B2PLYP-D3 (6%), though some of them (ωB97X, M06-2X and M11) are not able to describe an attractive interaction between PhF and benzene. Few other functionals present only slightly larger errors, namely, B97-D (16%), APF-D (16%), M05-2X (17%) and B2PLYP-D (13%), whose performance is then comparable to that of MP2 (16%). It is to be noted that the recently developed D3 add-on correction term[56] represents a remarkable improvement with respect to the D one.[54]

When looking at Figure 4, on the other hand, it appears that not exactly the same best functionals, i.e., those characterized by $<\varepsilon>_{\Delta Ecp} < 0.10$, are also able to reproduce the reference QTAIM properties with errors smaller than 10%. They are APF-D (6%), ωB97X (9%), M05-2X (8%), M06-2X (10%), M11 (4%), B2PLYP-D (6%), B2PLYP-D3 (8%) and mPW2PLYP-D (8%), with M11 showing the highest accuracy, comparable to that of MP2 (4%). Among them, APF-D, M05-2X and B2PLYP-D show a very good performance for the determination of topological properties but are not so good for evaluation of interaction energies, similar to MP2. The opposite behavior is found for B97-D3 and ωB97X-D, providing low $<\varepsilon>_{\Delta Ecp}$ errors but moderate (about 15%) percentage errors in the determination of the topological properties. In conclusion, only ωB97X, M06-2X, M11, mPW2PLYP-D and B2PLYP-D3 functionals are able to accurately reproduce both the reference properties.

All the other functionals reproduce very badly the binding energies as well as the QTAIM properties, though in general smaller errors are obtained for the latter. As already mentioned,

B3LYP and B3PWB91 are not able to describe any attractive interaction for the dimers involving the PhX molecule, and the errors for the dimers involving the NCX moiety are about 36% for the binding energy and 25% for the QTAIM properties. Even larger errors are obtained for the remaining functionals, that is, PBE1PBE (64%, 39% for percentage $<\mathcal{E}>_{\Delta Ecp}$, $<\mathcal{E}>_{QTAIM}$ errors, respectively), APF (73%, 45%), MPW2PLYP (46%, 32%) and B2PLYP (62%, 37%). It is clearly evident that the inclusion of the dispersion term is crucial also to well reproduce the QTAIM properties, besides the binding energies. The definite improvement from APF to APF-D, from B2PLYP to B2PLYP-D or B2PLYP-D3 and from MPW2PLYP to mPW2PLYP-D is in fact noted also by looking at the $<\mathcal{E}>_{QTAIM}$ errors, and the anomaly of the pair ωB97X/ωB97X-D is confirmed. Finally, contrarily to what found for the binding energies, a slightly better description of the topological properties is provided by the D dispersion correction term with respect to the D3 one.

4. CONCLUSIONS

The performance of different DFT functionals for the study of the DX/π halogen bonding interaction has been here tested by joined analysis of average errors on both binding energies and topological properties determined at bond critical points according to QTAIM. The averages were performed on DX/π dimers with D = NC and Ph, and all halogen atoms X = F, Cl, Br and I. Owing to the mixed dispersive and electrostatic nature of the DX/π halogen bonding, it resulted that functionals which correctly describe the dispersion correction are mandatory to accurately reproduce energetic and topological properties, though not the same functionals show the better performance for both sets of properties. The recommended functionals to investigate the present interaction are shown to be ωB97X, M06-2X, M11, mPW2PLYP-D and B2PLYP-D3, the latter

two presenting however higher computational costs with respect to the former ones owing to their double hybrid nature. The best functionals are able to reproduce the QTAIM properties with accuracy comparable with that of MP2, which, on the other hand, is here confirmed to be not suitable for the determination of accurate DX/π interaction energies. The worse performance in both energetic and topological properties is shown by the hybrid GGA functionals, including in particular the B3LYP and B3PW91 functionals, whose use is then strongly discouraged for studying the DX/π halogen bonding interaction.

■ ASSOCIATED CONTENT

Supporting Information

Counterpoise-corrected interaction energies, equilibrium distances and topological properties at the BCPs for all the investigated dimers. This material is available free of charge via the Internet at http://pubs.acs.org.

■ AUTHOR INFORMATION

Corresponding Authors

*E-mails: alessandra.forni@istm.cnr.it; stefano.pieraccini@unimi.it; maurizio.sironi@unimi.it

Notes

The authors declare no competing financial interest.

■ ACKNOWLEDGMENTS

We acknowledge the financial contribution from Fondazione della Banca del Monte di Lombardia.

■ REFERENCES

1. Steed, J. W.; Atwood, J. L. *Supramolecular Chemistry*, 2nd ed.; Wiley: Weinheim, Germany, **2009**.

2. Gilday, L. C.; Robinson, S. W.; Barendt, T. A.; Langton, M. J.; Mullaney, B. R.; Beer, P. D. Halogen Bonding in Supramolecular Chemistry. *Chem. Rev.* **2015**, *115*, 7118−7195.

3. Cavallo, G.; Metrangolo, P.; Milani, R.; Pilati, T.; Priimagi, A.; Resnati, G.; Terraneo, G. The Halogen Bond. *Chem. Rev.* **2016**, *116*, 2478−2601.

4. Fourmigué M.; Batail, P. Activation of Hydrogen- and Halogen-Bonding Interactions in Tetrathiafulvalene-Based Crystalline Molecular Conductors. *Chem. Rev.* **2004**, *104*, 5379−5418.

5. Hulliger, J.; Langley, P. J. On Intrinsic and Extrinsic Defect-Forming Mechanisms Determining the Disordered Structure of 4-Iodo-4′-Nitrobiphenyl Crystals. *Chem. Commun.* **1998**, 2557−2558.

6. Sarma, J. A. R. P.; Allen, F. H.; Hoy, V. J.; Howard, J. A. K.; Thaimattam, R.; Biradha, K.; Desiraju, G. R. Design of an SHG-Active Crystal, 4-iodo-4′-nitrobiphenyl: the Role of Supramolecular Synthons. *Chem. Commun.* **1997**, 101−102.

7. Thallapally, P. K.; Desiraju, G. R.; Bagieu-Beucher, M.; Masse, R.; Bourgogne, C.; Nicoud, J.-F. 1,3-Dibromo-2,4,6-trinitrobenzene (DBTNB). Crystal Engineering and Perfect

Polar Alignment of Two-dimensional Hyperpolarizable Chromophores. *Chem. Commun.* **2002**, 1052−1053.

8. Cariati, E.; Forni, A.; Biella, S.; Metrangolo, P.; Meyer, F.; Resnati, G.; Righetto, S.; Tordin, E.; Ugo, R. Tuning Second-Order NLO Responses through Halogen Bonding. *Chem. Commun.* **2007**, 2590−2592.

9. Cariati, E.; Cavallo, G.; Forni, A.; Leem, G.; Metrangolo, P.; Meyer, F.; Pilati, T.; Resnati, G.; Righetto, S.; Terraneo, G.; Tordin, E. Self-Complementary Nonlinear Optical-Phores Targeted to Halogen Bond-Driven Self-Assembly of Electro-Optic Materials. *Cryst. Growth Des.* **2011**, *11*, 5642−5648.

10. Farina, A.; Meille, S. V.; Messina, M. T.; Metrangolo, P.; Resnati, G.; Vecchio, G. Resolution of Racemic 1,2-Dibromohexafluoropropane through Halogen-Binded Supramolecular Helices. *Angew. Chem., Int. Ed.* **1999**, *38*, 2433−2436.

11. Walter, S. M.; Kniep, F.; Herdtweck, E.; Huber, S. M. Halogen-Bond-Induced Activation of a Carbon-Heteroatom Bond. *Angew. Chem., Int. Ed.* **2011**, *50*, 7187−7191.

12. Kniep, F.; Rout, L.; Walter, S. M.; Bensch, H. K. V.; Jungbauer, S. H.; Herdtweck, E.; Huber, S. M. 5-Iodo-1,2,3-Triazolium-Based Multidentate Halogen-Bond Donors as Activating Reagents. *Chem. Commun.* **2012**, *48*, 9299−9301.

13. Kniep, F.; Walter, S. M.; Herdtweck, E.; Huber, S. M. 4,4′-Azobis(halopyridinium) Derivatives: Strong Multidentate Halogen-Bond Donors with a Redox-Active Core. *Chem. - Eur. J.* **2012**, *18*, 1306−1310.

14. Jungbauer, S. H.; Walter, S. M.; Schindler, S.; Rout, L.; Kniep, F.; Huber, S. M. Activation of a Carbonyl Compound by Halogen Bonding. *Chem. Commun.* **2014**, *50*, 6281−6284.

15. Dove, A. P.; Pratt, R. C.; Lohmeijer, B. G. G.; Waymouth, R. M.; Hedrick, J. L. Thiourea-Based Bifunctional Organocatalysis: Supramolecular Recognition for Living Polymerization *J. Am. Chem. Soc.* **2005**, *127*, 13798-13799.

16. Dordonne, S.; Crousse, B.; Bonnet-Delpon, D.; Legros, J. Fluorous Tagging of DABCO through Halogen Bonding: Recyclable Catalyst for the Morita-Baylis-Hillman Reaction. *Chem. Commun.* **2011**, *47*, 5855−5857.

17. Alcaide, B.; Almendros, P.; Cabrero, G.; Ruiz, M. P. Direct Synthesis of Protected Enantiopure 5-Cyano-3,4-Dihydroxypyrrolidin-2-Ones from β-Lactam Aldehydes Catalyzed by Iodine. *Synthesis* **2008**, *2008*, 2835−2839.

18. Beale, T. M.; Chudzinski, M. G.; Sarwar, M. G.; Taylor, M. S. Halogen Bonding in Solution: Thermodynamics and Applications. *Chem. Soc. Rev.* **2013**, *42*, 1667−1680.

19. Mele, A.; Metrangolo, P.; Neukirch, H.; Pilati, T.; Resnati, G. A Halogen-Bonding-Based Heteroditopic Receptor for Alkali Metal Halides. *J. Am. Chem. Soc.* **2005**, *127*, 14972−14973.

20. Mínguez Espallargas, G.; Brammer, L.; van de Streek, J.; Shankland, K.; Florence, A. J.; Adams, H. Reversible Extrusion and Uptake of HCl Molecules by Crystalline Solids Involving Coordination Bond Cleavage and Formation. *J. Am. Chem. Soc.* **2006**, *128*, 9584−9585.

21. Lu, Y.; Wang, Y.; Zhu, W. Nonbonding Interactions of Organic Halogens in Biological Systems: Implications for Drug Discovery and Biomolecular Design. *Phys. Chem. Chem. Phys.* **2010**, *12*, 4543−4551.

22. Voth, A. R.; Hays, F. A.; Ho, P. S. Directing Macromolecular Conformation through Halogen Bonds. *Proc. Natl. Acad. Sci. U. S. A.* **2007**, *104*, 6188−6193.

23. Clark, T.; Hennemann, M.; Murray, J. S.; Politzer, P. Halogen Bonding: The Sigma-Hole. *J. Mol. Model.* **2007**, *13*, 291−296.

24. Politzer, P.; Lane, P.; Concha, M. C.; Ma, Y.; Murray, S. An Overview of Halogen Bonding. *J. Mol. Model.* **2007**, *13*, 305-311.

25. Riley, K. E.; Murray, J. S.; Politzer, P.; Concha, M. C.; Hobza, P. Br···O Complexes as Probes of Factors Affecting Halogen Bonding: Interactions of Bromobenzenes and Bromopyrimidines with Acetone. *J. Chem. Theory Comput.* **2009**, *5*, 155-163.

26. Eskandari, K.; Zariny, H. Halogen Bonding: A Lump-Hole Interaction. *Chem. Phys. Lett.* **2010**, *492*, 9-13.

27. Bader, R. F. W. Atoms in Molecules: a Quantum Theory. International Series of Monographs on Chemistry 22, Oxford University Press, Oxford, **1990**.

28. Tognetti, V.; Joubert, L. Electron Density Laplacian and Halogen Bonds. *Theor. Chem. Acc.* **2015**, *134*, 90.

29. Koritsanszky, T. S.; Coppens, P. Chemical Applications of X-ray Charge-Density Analysis. *Chem. Rev.* **2001**, *101*, 1583-1627.

30. Duarte, D. J. R.; Sosa, G. L.; Peruchena, N. M.; Alkorta, I. Halogen Bonding. The role of the Polarizability of the Electron-Pair Donor. *Phys. Chem. Chem. Phys.* **2016**, *18*, 7300-7309.

31. Kolář, M. H.; Hobza, P. Computer Modeling of Halogen Bonding and Other σ-Hole Interactions. *Chem. Rev.* **2016**, *116*, 5155-5187.

32. Kozuch, S.; Martin, J.M.L. Halogen Bonds: Benchmarks and Theoretical Analysis. *J. Chem. Theory Comput*. **2013**, *9*, 1918-1931.

33. Forni, A.; Rendine, S.; Pieraccini, S.; Sironi, M. Solvent Effect on Halogen Bonding: The Case of the I···O Interaction. *J. Mol. Graph. Mod.* **2012**, *38*, 31-39.

34. Sure, R.; Grimme, S. Comprehensive Benchmark of Association (Free) Energies of Realistic Host−Guest Complexes. *J. Chem. Theory Comput*. **2015**, *11*, 3785-3801.

35. Liu, F.; Du, L.; Zhang, D.; Gao, J. Performance of Density Functional Theory on the Anisotropic Halogen…Halogen Interactions and Potential Energy Surface: Problems and Possible Solutions. *Int. J. Quantum Chem*. **2016**, *116*, 710-717.

36. Lu, Y.; Zou, J.; Wang, Y.; Jiang, Y.; Yu, Q. Ab Initio Investigation of the Complexes between Bromobenzene and Several Electron Donors: Some Insights into the Magnitude and Nature of Halogen Bonding Interactions. *J. Phys. Chem. A* **2007**, *111*, 10781−10788.

37. Amezaga, N. J. M.; Pamies, S. C.; Peruchena, N. M.; Sosa, G. L. Halogen Bonding: a Study Based on the Electronic Charge Density. *J. Phys. Chem. A* **2010**, *114*, 552–562.

38. Zhang, X.; Zeng, Y.; Li, X.; Meng, L.; Zheng, S. A Computational Study on the Nature of the Halogen Bond between Sulfides and Dihalogen Molecules. *Struct. Chem*. **2011**, *22*, 567–576.

39. Duarte, D. J. R.; Angelina, E. L.; Peruchena, N. M. On the Strength of the Halogen Bonds: Mutual Penetration, Atomic Quadrupole Moment and Laplacian Distribution of the Charge Density Analyses. *Comput. Theor. Chem*. **2012**, *998*, 164–172.

40. Grabowski, S. J. QTAIM Characteristics of Halogen Bond and Related Interactions. *J. Phys. Chem. A* **2012**, *116*, 1838–1845.

41. Forni, A.; Pieraccini, S.; Rendine, S.; Gabas, F.; Sironi, M. Halogen-Bonding Interactions with π Systems: CCSD(T), MP2, and DFT Calculations. *ChemPhysChem* **2012**, *13*, 4224 – 4234.

42. Syzgantseva, O. A.; Tognetti, V.; Joubert, L. On the Physical Nature of Halogen Bonds: a QTAIM Study. *J. Phys. Chem A* **2013**, *117*, 8969–8980.

43. Yahia-Ouahmed, M.; Tognetti, V.; Joubert, L. Halogen–Halogen Interactions in Perhalogenated Ethanes: an Interacting Quantum Atoms Study. *Comput. Theor. Chem.* **2015**, *1053*, 254–262.

44. Albrecht, L.; Boyd, R. J.; Mó, O.; Yáñez, M. Changing Weak Halogen Bonds into Strong Ones through Cooperativity with Beryllium Bonds. *J. Phys. Chem. A* **2014**, *118*, 4205–4213.

45. Forni, A. Experimental and Theoretical Study of the Br···N Halogen Bond in Complexes of 1,4-Dibromotetrafluorobenzene with Dipyridyl Derivatives. *J. Phys. Chem. A* **2009**, *113*, 3403−3412.

46. Eskandari, K.; Lesani, M. Does Fluorine Participate in Halogen Bonding? *Chem. - Eur. J.* **2015**, *21*, 4739−4746.

47. Tognetti, V.; Joubert, L. On the Influence of Density Functional Approximations on Some Local Bader's Atoms-in-Molecules Properties. *J. Phys. Chem. A* **2011**, *115*, 5505–5515.

48. Forni, A.; Pieraccini, S.; Rendine, S.; Sironi, M. Halogen Bonds with Benzene: An Assessment of DFT Functionals. *J. Comp. Chem.* **2014**, *35*, 386–394.

49. Xu, Z.; Yang, Z.; Liu, Y.; Lu, Y.; Chen, K.; Zhu, W. Halogen Bond: Its Role beyond Drug-Target Binding Affinity for Drug Discovery and Development. *J. Chem. Inf. Model.* **2014**, *54*, 69−78.

50. Matter, H.; Nazar, M.; Gussregen, S.; Will, D. W.; Schreuder, H.; Bauer, A. Evidence for C–Cl/C–Br···π Interactions as an Important Contribution to Protein–Ligand Binding Affinity. *Angew. Chem. Int. Ed.* **2009**, 48, 2911-2916.

51. Peterson, K. A.; Shepler, B. C.; Figgen, D.; Stoll, H. On the Spectroscopic and Thermochemical Properties of ClO, BrO, IO, and Their Anions. *J. Phys. Chem. A* **2006**, *110*, 13877–13883.

52. Johnson, E. R.; Wolkow, R. A.; DiLabio, G. A. Application of 25 Density Functionals to Dispersion-Bound Homomolecular Dimers. *Chem. Phys. Lett.* **2004**, *394*, 334-338.

53. Johnson, E. R.; Becke, A. D.; Sherrill, C. D.; DiLabio G. A. Oscillations in Meta-Generalized-Gradient Approximation Potential Energy Surfaces for Dispersion-Bound Complexes. *J. Chem. Phys.* **2009**, *131*, 034111.

54. Grimme, S. Semiempirical GGA-Type Density Functional Constructed with a Long-Range Dispersion Correction *J. Comp. Chem.* **2006**, *27*, 1787-1799.

55. Becke, A. D. Density-Functional Thermochemistry. V. Systematic Optimization of Exchange-Correlation Functionals. *J. Chem. Phys.* **1997**, *107*, 8554-8560.

56. Grimme, S.; Antony, J.; Ehrlich, S.; Krieg, H. A Consistent and Accurate Ab Initio Parametrization of Density Functional Dispersion Correction (DFT-D) for the 94 Elements H-Pu. *J. Chem. Phys*. **2010**, *132*, 154104.

57. Grimme, S.; Ehrlich S.; Goerigk, L. Effect of the Damping Function in Dispersion Corrected Density Functional Theory. *J. Comp. Chem.* **2011**, *32*, 1456-1465.

58. Lee, C.; Yang, W.; Parr, R. G. Development of the Colle-Salvetti Correlation-Energy Formula into a Functional of the Electron Density. *Phys. Rev. B* **1988**, *37*, 785-789.

59. Becke, A. D. Density-Functional Thermochemistry. III. The Role of Exact Exchange. *J. Chem. Phys.* **1993**, *98*, 5648-5652.

60. Vosko, S. H.; Wilk, L.; Nusair, M. Accurate Spin-Dependent Electron Liquid Correlation Energies for Local Spin Density Calculations: a Critical Analysis. *Can. J. Phys.* **1980**, *58*, 1200-1211.

61. Perdew, J. P.; Chevary, J. A.; Vosko, S. H.; Jackson, K. A.; Pederson, M. R.; Singh, D. J.; Fiolhais, C. Atoms, Molecules, Solids, and Surfaces: Applications of the Generalized Gradient Approximation for Exchange and Correlation. *Phys. Rev. B* **1992**, *46*, 6671−6687.

62. Perdew, J. P.; Chevary, J. A.; Vosko, S. H.; Jackson, K. A.; Pederson, M. R.; Singh, D. J.; Fiolhais, C. Erratum: Atoms, Molecules, Solids, and Surfaces - Applications of the Generalized Gradient Approximation for Exchange and Correlation. *Phys. Rev. B* **1993**, *48*, 4978−4978.

63. Perdew, J. P.; Burke, K.; Ernzerhof, M. Generalized Gradient Approximation Made Simple. *Phys. Rev. Lett.* **1996**, *77*, 3865-3868.

64. Adamo, C.; Barone, V. Toward Reliable Density Functional Methods without Adjustable Parameters: The PBE0 model. *J. Chem. Phys.* **1999**, *110*, 6158-6169.

65. Austin, A.; Petersson, G. A.; Frisch, M. J.; Dobek, F. J.; Scalmani, G.; Throssell, K. A Density Functional with Spherical Atom Dispersion Terms. *J. Chem. Theory Comput.* **2012**, *8*, 4989–5007.

66. Chai, J. D.; Head-Gordon, M. Systematic Optimization of Long-Range Corrected Hybrid Density Functionals. *J. Chem. Phys.* **2008**, *128*, 084106.

67. Chai, J. D.; Head-Gordon, M. Long-Range Corrected Hybrid Density Functionals with Damped Atom–Atom Dispersion Corrections. *Phys. Chem. Chem. Phys.* **2008**, *10*, 6615-6620.

68. Zhao, Y.; Schultz, N. E.; Truhlar, D.G. Design of Density Functionals by Combining the Method of Constraint Satisfaction with Parametrization for Thermochemistry, Thermochemical Kinetics, and Noncovalent Interactions. *J. Chem. Theory Comput.* **2006**, *2*, 364-382.

69. Zhao, Y.; Truhlar, D.G. The M06 Suite of Density Functionals for Main Group Thermochemistry, Thermochemical Kinetics, Noncovalent Interactions, Excited States, and Transition Elements: Two New Functionals and Systematic Testing of Four M06-Class Functionals and 12 Other Functionals. *Theor. Chem. Acc.* **2008**, *120*, 215-241.

70. Peverati R.; Truhlar, D. G. Improving the Accuracy of Hybrid Meta-GGA Density Functionals by Range Separation. *J. Phys. Chem. Lett.* **2011**, *2*, 2810-2817.

71. Becke, A. D. Density-Functional Exchange-Energy Approximation with Correct Asymptotic Behavior. *Phys. Rev. A* **1988**, *38*, 3098-3100.

72. Grimme, S. Semiempirical Hybrid Density Functional with Perturbative Second-Order Correlation. *J. Chem. Phys.* **2006**, *124*, 034108.

73. Adamo, C.; Barone, V. Exchange Functionals with Improved Long-Range Behavior and Adiabatic Connection Methods without Adjustable Parameters: The mPW and mPW1PW Models. *J. Chem. Phys.* **1998**, *108*, 664-675.

74. Schwabe, T.; Grimme, S. Towards Chemical Accuracy for the Thermodynamics of Large Molecules: New Hybrid Density Functionals Including Non-Local Correlation Effects. *Phys. Chem. Chem. Phys.* **2006**, *8*, 4398-4401.

75. Schwabe, T.; Grimme, S. Double-Hybrid Density Functionals with Long-Range Dispersion Corrections: Higher Accuracy and Extended Applicability. *Phys. Chem. Chem. Phys.* **2007**, *9*, 3397-3406.

76. Smith, D. G. A.; Burns, L. A.; Patkowski, K.; Sherrill, C. D. Revised Damping Parameters for the D3 Dispersion Correction to Density Functional Theory. *J. Phys. Chem. Lett.* **2016**, *7*, 2197−2203.

77. Bader, R. F. W.; Essen, H. The Characterization of Atomic Interactions. *J. Chem. Phys.* **1984**, *80*, 1943 –1960.

78. Espinosa, E.; Alkorta, I.; Elguero, J.; Molins, E. From Weak to Strong Interactions: A Comprehensive Analysis of the Topological and Energetic Properties of the Electron Density Distribution Involving X–H···F–Y Systems. *J. Chem. Phys.* **2002**, *117*, 5529 –5542.

79. Lippmann, T.; Schneider, J. R. Topological Analyses of Cuprite, Cu2O, Using High-Energy Synchrotron-Radiation Data. *Acta Crystallogr. Sect. A* **2000**, *56*, 575 –584.

80. Frisch, M. J.; Trucks, G. W.; Schlegel, H. B.; Scuseria, G. E.; Robb, M. A.; Cheeseman, J. R.; Scalmani, G.; Barone, V.; Mennucci, B.; Petersson, G. A.; Nakatsuji, H.; Caricato, M.; Li, X.; Hratchian, H. P.; Izmaylov, A. F.; Bloino, J.; Zheng, G.; Sonnenberg, J. L.; Hada, M.; Ehara, M.; Toyota, K.; Fukuda, R.; Hasegawa, J.; Ishida, M.; Nakajima, T.; Honda, Y.; Kitao, O.; Nakai, H.; Vreven, T.; Montgomery, J. A., Jr.; Peralta, J. E.; Ogliaro, F.; Bearpark, M.; Heyd, J. J.; Brothers, E.; Kudin, K. N.; Staroverov, V. N.; Kobayashi, R.; Normand, J.; Raghavachari, K.; Rendell, A.; Burant, J. C.; Iyengar, S. S.; Tomasi, J.; Cossi, M.; Rega, N.; Millam, J. M.; Klene, M.; Knox, J. E.; Cross, J. B.; Bakken, V.; Adamo, C.; Jaramillo, J.; Gomperts, R.; Stratmann, R.

E.; Yazyev, O.; Austin, A. J.; Cammi, R.; Pomelli, C.; Ochterski, J. W.; Martin, R. L.; Morokuma, K.; Zakrzewski, V. G.; Voth, G. A.; Salvador, P.; Dannenberg, J. J.; Dapprich, S.; Daniels, A. D.; Farkas, Ö.; Foresman, J. B.; Ortiz, J. V.; Cioslowski, J.; Fox, D. J. Gaussian 09, Revision D.01 Gaussian, Inc., Wallingford CT, 2013.

81. Keith, T. A. AIMAll (Version 12.05.09), TK Gristmill Software, Overland Park KS, USA, 2012, http://aim.tkgristmill.com.

82. Tognetti, V.; Joubert, L.; Raucoules, R.; De Bruin, T.; Adamo, C. Characterizing Agosticity Using the Quantum Theory of Atoms in Molecules: Bond Critical Points and Their Local Properties. *J. Phys. Chem. A* **2012**, *116*, 5472−5479.

83. Rodríguez, J. I.; Ayers, P. W.; Götz, A. W.; Castillo-Alvarado, F. L. *J. Chem. Phys.* **2009**, *131*, 021101.

84. Patrikeev, L.; Joubert, L.; Tognetti, V. Atomic Decomposition of Kohn–Sham Molecular Energies: The Kinetic Energy Component. *Mol. Phys.* **2016**, *114*, 1285−1296.

85. Tognetti, V.; Joubert, L. Density Functional Theory and Bader's Atoms-In-Molecules Theory: Towards a Vivid Dialogue. *Phys. Chem. Chem. Phys.* **2014**, *16*, 14539−14550.

86. Metrangolo, P.; Murray, J. S.; Pilati, T.; Politzer, P.; Resnati, G.; Terraneo, G. Fluorine-Centered Halogen Bonding: A Factor in Recognition Phenomena and Reactivity. *Cryst. Growth Des*. **2011**, *11*, 4238–4246.

87. Wang, Y.; Tong, J.; Wu, W.; Xu, Z.; Lu, Y. Organic Fluorines as Halogen Bond Donors: Theoretical Study and Crystallographic Evidence. *Int. J. Quantum Chem.* **2015**, *115*, 884–890.

88. Grabowski, S. J.; Ugalde, J. M. Bond Paths Show Preferable Interactions: Ab Initio and QTAIM Studies on the X-H· · ·π Hydrogen Bond. *J. Phys. Chem. A* **2010**, *114*, 7223–7229.

89. Nishio, M. The CH/π Hydrogen Bond in Chemistry. Conformation, Supramolecules, Optical Resolution and Interactions Involving Carbohydrates. *Phys. Chem. Chem. Phys.* **2011**, *13*, 13873– 13900.

90. Ran, J.; Wong, M. W. Saturated Hydrocarbon−Benzene Complexes: Theoretical Study of Cooperative CH/π Interactions. *J. Phys. Chem. A* **2006**, *110*, 9702 –9709.

91. Sherrill, C. D. Computations of Noncovalent π Interactions. *Rev. Comput. Chem.* **2009**, *26*, 1-38.

92. Otero-de-la-Roza, A.; Johnson, E. R.; DiLabio, G. A. Halogen Bonding from Dispersion-Corrected Density-Functional Theory: The Role of Delocalization Error. *J. Chem. Theory Comput.* **2014**, *10*, 5436-5447.

93. Becke, A. D.; Johnson, E. R. Exchange-Hole Dipole Moment and the Dispersion Interaction. *J. Chem. Phys*. **2005**, *122*, 154104.

94. Becke, A. D.; Johnson, E. R. Exchange-Hole Dipole Moment and the Dispersion Interaction Revisited. *J. Chem. Phys*. **2007**, *127*, 154108.

Table of Contents Graphic and Synopsis

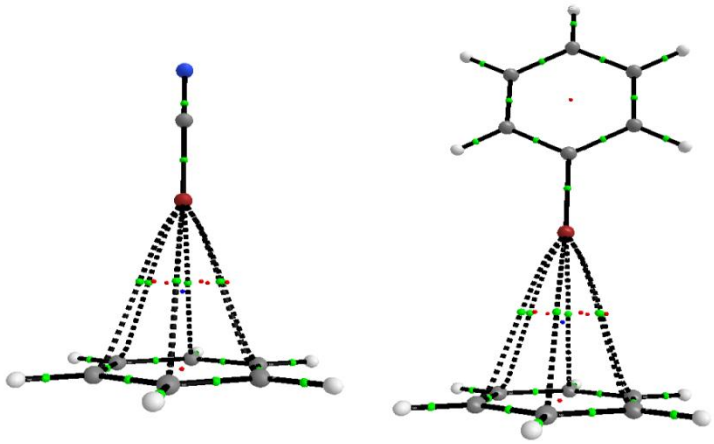

A detailed analysis of the performance of an extensive set of DFT functionals in reproducing accurate binding energies and topological properties for the halogen bonding interaction of either NCX or PhX molecules (X = F, Cl, Br, I) with the aromatic system of benzene in the T-shaped configuration is here reported.